The Astrophysical Journal Letters, 738:L20 (6pp), 2011 September 10 doi:10.1088/2041-8205/738/2/L20

A MICRO CORONAL MASS EJECTION ASSOCIATED BLOWOUT EXTREME-ULTRAVIOLET JET

Junchao Hong, Yunchun Jiang, Ruisheng Zheng, Jiayan Yang, Yi Bi, and Bo Yang
National Astronomical Observatories/Yunnan Astronomical Observatory, Chinese Academy of Sciences, Kunming 650011, China; hjcsolar@ynao.ac.cn
Received 2011 July 7; accepted 2011 August 1; published 2011 August 17

ABSTRACT

The so-called mini coronal mass ejections (CMEs) were recently identified as small-scale eruptive events showing the same on-disk characteristics as large-scale CMEs, and Moore et al. further found that one-third of polar X-ray jets are the so-called blowout jets, in which the jet-base magnetic arch, often carrying a filament, undergoes a miniature version of the blowout eruptions that produce major CMEs. By means of the two viewpoint observations from the *Solar Dynamics Observatory* (*SDO*) and the *Ahead of Solar Terrestrial Relations Observatory* (*STEREO A*), in this Letter, we present the first observations that a blowout jet from the eruption of an EUV mini-filament channel in the quiet Sun was indeed associated with a real micro-CME. Captured by the on-disk *SDO* observations, the whole life of the mini-filament channel, from the formation to eruption, was associated with convergences and cancellations of opposite-polarity magnetic flux in the photosphere, and its eruption was accompanied by a small flare-like brightening, a small corona dimming, and posteruptive loops. The near-limb counterpart of the eruption observed by *STEREO A*, however, showed up as a small EUV jet followed by a white-light jet. These observations not only confirm the previous results that mini-filaments have characteristics common to large-scale ones, but also give clear evidences that blowout jets can result from the eruptions of mini-filaments and are associated with mini-CME.

Key words: Sun: coronal mass ejections (CMEs) – Sun: filaments, prominences – Sun: surface magnetism

Online-only material: color figures

1. INTRODUCTION

Numerous small-scale eruptions frequently occur everywhere in the quiet Sun. Among masses of small-scale dynamic events are mini-filament eruptions, which are the small-scale analogs to large-scale ones often in association with two-ribbon flares and coronal mass ejections (CMEs; Hermans & Martin 1986). Along magnetic polarity reversal boundaries, miniature filaments show a curved or arch-like shape and have a mean projected length of only 19 Mm, and their eruptions are usually accompanied by magnetic flux cancellations in the photosphere, tiny flare ribbons similar to those in large-scale filament eruptions, small coronal dimmings, and so on (Wang et al. 2000; Sakajiri et al. 2004; Ren et al. 2008). Therefore, small-scale filament eruptions have common properties similar to their large-scale counterparts; this strongly implies that some of them should relate to CMEs (Schrijver 2010). Innes et al. (2009) and Podladchikova et al. (2010) gave several examples of the so-called mini-CMEs only exhibiting the same on-disk signatures and characteristics as large-scale CMEs, but no associated small white-light CME was really observed. As a result, no miniature filament eruption was reported to be associated with small-scale CME up until now, and high-resolution observations are needed to clarify this possibility.

Some previous observations showed that activations or eruptions of small-scale filaments can be physically related with collimated plasma ejections, which show up as surges in Hα and jets in EUV and X-ray (Chae et al. 1999; Jiang et al. 2007; Zuccarello et al. 2007). Different from standard X-ray jets that fit the standard reconnection picture for coronal jets, Moore et al. (2010) recently found that one-third of X-ray jets are the so-called blowout jets, in which the jet-base magnetic arch often carries a filament, and they do have enough shear and twist to undergo a miniature version of the blowout eruptions that produce major CMEs. This means that part of small-scale filaments can erupt as jets. Therefore, it is very likely that, as the outward extensions of EUV jets, part of coronal white-light jets (Wang et al. 1998; Wang & Sheeley 2002; Paraschiv et al. 2010) are indeed small-scale CMEs from blowout jets, i.e., eruptions of mini-filaments.

On 2010 July 19, an EUV mini-filament channel erupted on the disk, and the entire process from its formation to eruption was well covered by observations from the *Solar Dynamics Observatory* (*SDO*; Schwer et al. 2002) with high spatial and temporal resolutions. Fortunately, the corresponding eruption, showing up as an EUV and white-light jet near the East limb, was observed by the Extreme Ultraviolet Imager (EUVI; Wuelser et al. 2004) and the Inner Coronagraphs (COR1; Thompson et al. 2010) on board the *Ahead of Solar Terrestrial Relations Observatory* (*STEREO A*). The simultaneous images form two different views and thus enable us to easily identify the eruption as a blowout jet that actually led to a jet-like CME.

2. OBSERVATIONS

In the field of view (FOV) of *SDO*, the eruptive EUV mini-filament channel was located in a quiet region close to the center of the solar disk (E2°N14°). To detail the eruption, we adopt full-disk EUV images from the Atmospheric Imaging Assembly (AIA; Boerner et al. 2010) and line-of-sight magnetograms from the Helioseismic and Magnetic Imager (HMI; Schou et al. 2010) on board *SDO*. AIA takes multi-wavelength images with a pixel size of 0.″6 and a 12 s cadence. We focus on the 304 Å (He II; $\log T = 4.7$), 193 Å (Fe XII (XXIV); $\log T = 6.1$), and 211 Å (Fe XIV; $\log T = 6.3$) images (Level 1.5) that mainly reveal information of the chromosphere and corona. HMI provides full-disk magnetograms observed in the Fe I 6173 Å absorption line, with a spatial sampling of 0.″5 pixel^{-1}, a 45 s cadence, and a noise level of approximately 10 G.

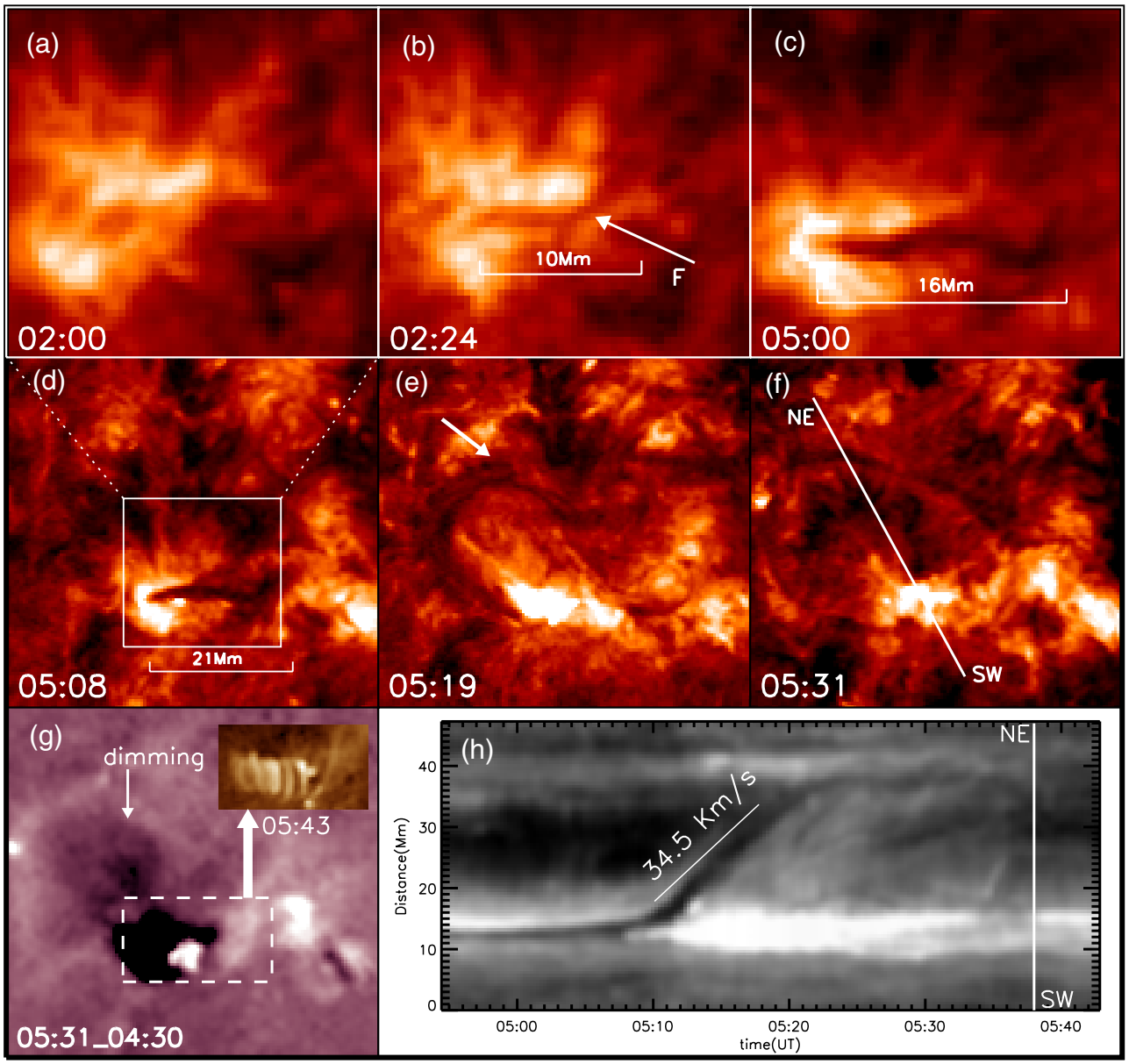

Figure 1. *SDO*/AIA EUV images (a)–(g) showing the evolution of the event. Panels (a)–(f) are direct 304 Å images showing the formation and eruption of a mini-filament, "F," while panel (g) is a 211 Å difference image, with an insert of a direct 193 Å image, showing the associated corona dimming and post-eruptive loops. The arrow in panel (e) indicates the erupting F, and the solid line in panel (f), pointing from SW to NE, marks the slit position of the time slice shown in panel (h). Time slice from 304 Å images showing the eruption trajectory of F, with the linear fitting to its outer edge marked as the solid line. The field of view (FOV) for panels (d)–(g) is $77'' \times 70''$, and $33'' \times 30''$ for panels (a)–(c), indicated by the white box in panel (d).

(A color version of this figure is available in the online journal.)

On 2010 July 19, *STEREO A* was about 77° ahead of the Earth and solar features near the solar disk from *SDO* were located close to the east limb from *STEREO A*. Therefore, the event was observed from the two nearly perpendicular perspectives of *SDO* and *STEREO A*. We identify the corresponding locations of events on two spacecraft by using a related code in SolarSoft which is usually used in reconstructing the three-dimensional structure of features from two viewpoint observations. To study the corresponding near-limb eruption, we examine full-disk 304 Å images from *STEREO A*/EUVI, with an FOV out to about 1.5 solar radii, a pixel resolution of 1.″6, and a cadence of 150 s. To identify the associated CME, observations from *STEREO A*/COR1 are also used. Having an FOV from 1.5 to 4 solar radii and a pixel resolution of 15″, COR1 images were available at a 5 minute cadence for our event.

3. RESULTS

Figure 1 shows the formation and eruption of an EUV mini-filament channel, "F," in AIA observations. Although the exact start time of F formation cannot be determined due to its very small size and changes in brightness, we can estimate its first appearance at about 02:24 UT from a AIA 304 Å movie. We see that F did not exist at 02:00 UT but appeared as a clear dark channel dividing two bright patches in 304 Å images by 02:24 UT. Consistent with the preferential pattern of dextral filament in the northern hemisphere (Zirker et al. 1997), it is noted that F showed a slight inverse-S shape with a near east–west orientation and a length of about 10 Mm. Afterward, F grew toward the west (see the 05:00 UT image) and reached its maximum extent with a projected length of about 21 Mm

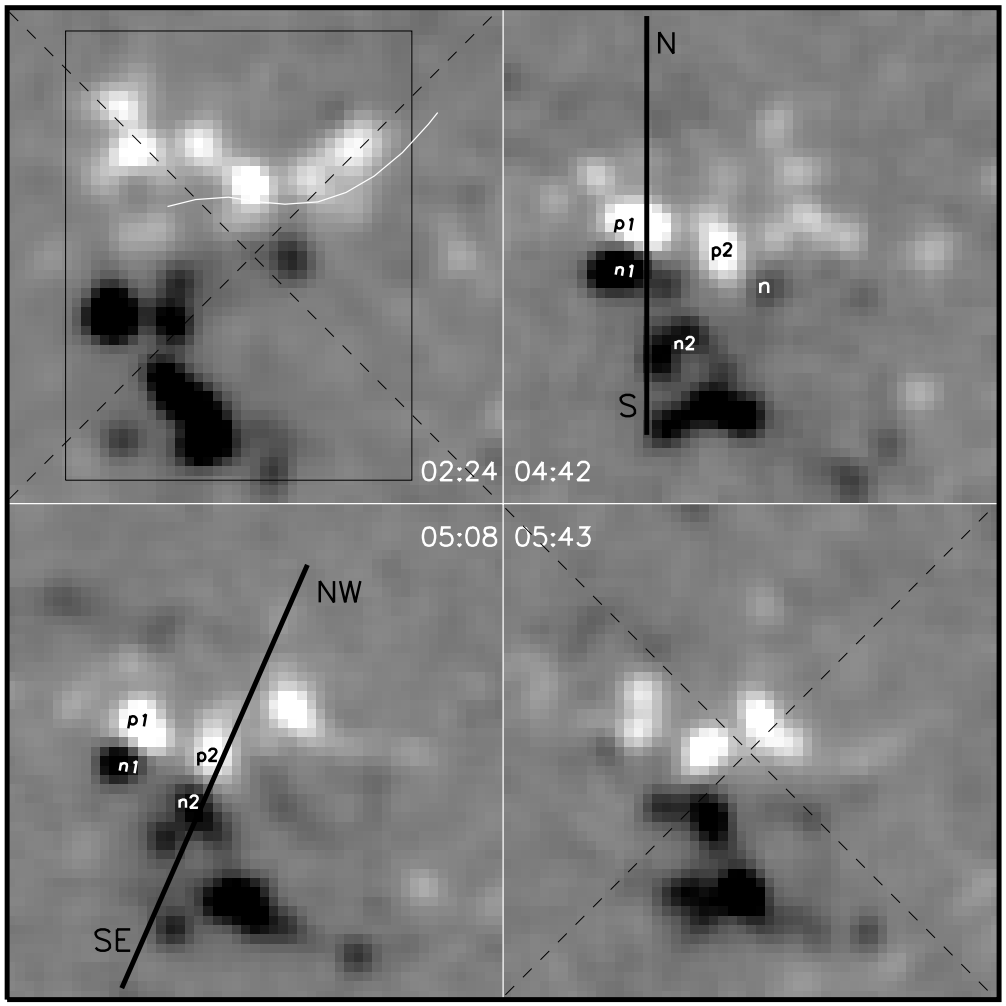

Figure 2. *SDO*/HMI magnetograms showing the evolution of photospheric magnetic field below F, with the outline of F's axis from the 02:24 UT AIA 304 Å image superposed as a white curve. Five positive and negative flux patches are denoted as "p1," "p2," "n1," "n2," and "n," and the diagonal-dashed lines help to show their movements and cancellations. The two thick black lines, pointing from S to N and SE to NW, respectively, mark the slit positions of the time slices given in Figure 3. The box indicates an area in which changes of magnetic flux are measured and plotted in Figure 3. The FOV is $26'' \times 26''$.

by about 05:08 UT. This was well consistent with the 19 Mm average projected length of miniature filaments given by Wang et al. (2000). Finally, the fully developed F underwent a drastic eruption from 05:08 UT and disappeared about after 05:43 UT. The F's top quickly lifted toward the northeastern direction (indicated by the white arrow in the 05:19 UT image) while its two ends remained fixed. As a result, the erupting F had a semi-circle shape. Since the eruptive region was near its central meridian passage in the northern hemisphere, taking the project effect into account, it is probable that F did not erupt vertically but had a non-radial path (Jiang et al. 2009; Bi et al. 2011). It is clear that such eruption was followed by pronounced flare-like brightening (see panels (d)–(f)). Although it was too compact to show a two-ribbon nature due to the extreme small scale of the eruptive F, post-eruptive loops clearly appeared to connect the brightening along the erupted F (see the inserted 05:43 UT 193 Å image). Similar to previous observations of small-scale eruption events (Ren et al. 2008; Innes et al. 2009), the F eruption was also accompanied by the formation of clear corona dimming at its northern side (see the 05:31 UT 211 Å difference image). To clearly display the F eruption, a time slice along a line passing over the top of the erupting F and its original centroid over time is taken from 304 Å images. The result is given in Figure 1(h), in which the erupting F appeared as a diagonal dark streak. We see that F nearly erupted at a constant projected velocity of about 34.5 km s^{-1} and was accompanied by the appearance of the brightening. Consistent with some previous observations (Wang et al. 2000; Sakajiri et al. 2004; Ren et al. 2008), therefore, the F eruption showed some distinct characteristics of active-region or quiet-region large-scale filament eruptions.

By inspecting HMI magnetic field observations, it is found that the formation and eruption of F were closely associated with convergences and then cancellations of opposite-polarity magnetic flux. Figure 2 presents HMI magnetograms in a window covering the eruptive region well. When the outlines of F's axis from the 02:24 UT 304 Å image was superimposed on the corresponding magnetogram, we found that F resided almost above the polarity inversion between several opposite-polarity flux patches. By comparing the first and last magnetograms, obvious flux convergences and cancellations were then manifested by the approaches and the decreasing areas of these opposite-polarity patches. Moreover, it is interesting to note that, besides the convergence motions, these flux patches also showed slightly shearing motions. The positive patches moved eastward while the negative ones moved westward. To show the convergences and cancellations, the five flux patches are labeled "p1," "n1,"

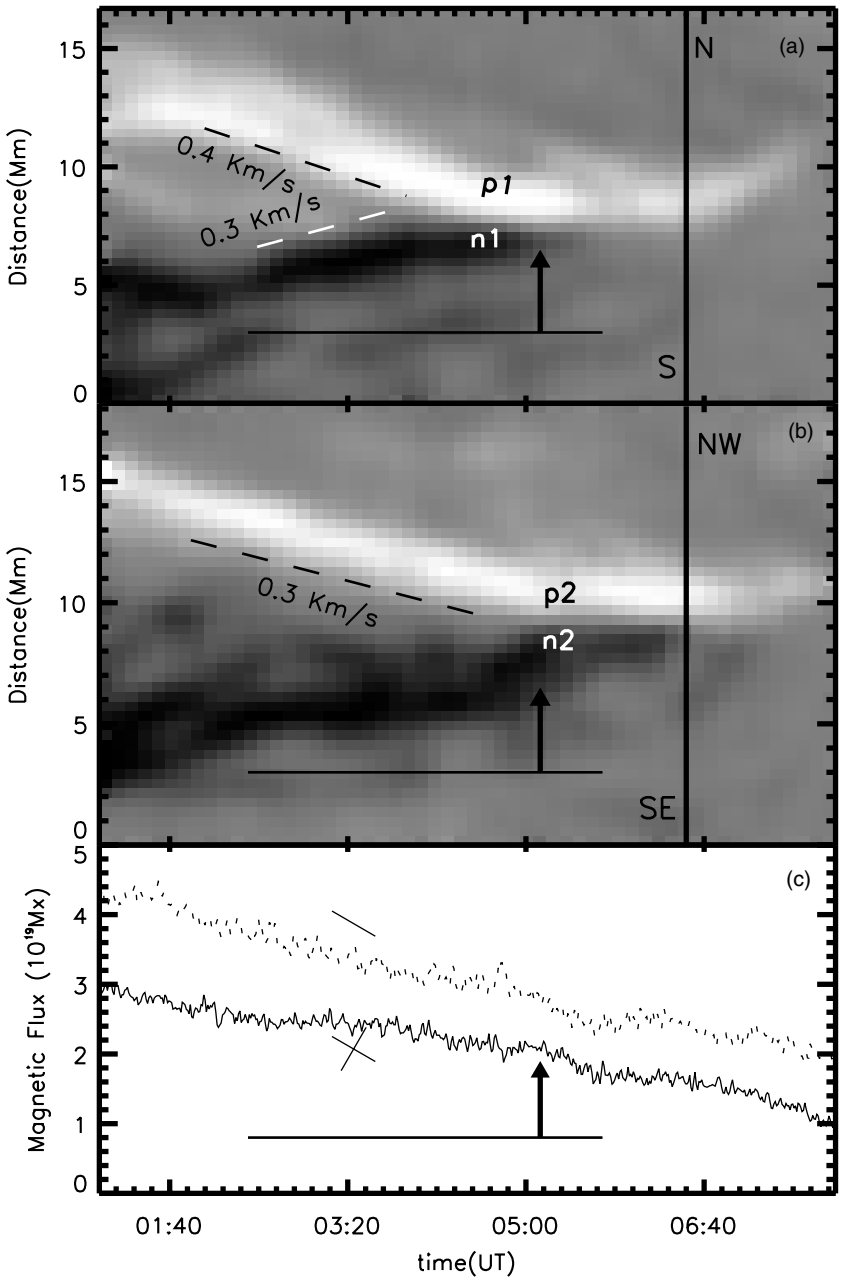

Figure 3. Time slices from HMI magnetograms for the two slits shown in Figures 2(a) and (b), and the changes in magnetic flux in the box area of Figure 2(c). The horizontal bars indicate the duration of the F formation and eruption, and the black arrows indicate the start time of the F eruption.

"p2," "n2," and "n." We see that they get closer to each other with time, and p1 met with n1 at 04:42 UT while p2 met with n and n2 at 04:42 and 05:08 UT, respectively. The areas of these patches continuously decreased after their meetings. At 05:08 UT when F started to erupt, n and part of n1 disappeared. By 05:43 UT after eruption, n1 almost completely disappeared and p1 became very weak. To more clearly display the above process, time slices along the two black lines, which exactly pass through p1/n1, p2/n2, as well as their meeting sites, are made from HMI magnetograms, and changes of the positive and negative flux within the black box covering the canceling flux patches are measured. In Figure 3, the results are given and compared with the times of the F formation and eruption. It is clear that p1–n1 and p2–n2 pairs converged to each other at constant speeds of about 0.3∼0.4 km s^{-1} during the F formation, then came into contact just before or at the F eruption start, and eventually underwent obvious flux loss or even disappeared during and after the eruption. This is consistent with that the positive and negative flux continuously decreased at a nearly uniform rate in the course of the F formation and eruption. These observations support the idea that convergence and cancellation of opposite-polarity magnetic fields not only are necessary conditions for the formation of filaments (Martin 1998) but also might play important roles in disturbing small filaments (Hermans & Martin 1986; Jiang & Wang 2001; Sakajiri et al. 2004; Ren et al. 2008).

Since the on-disk F eruption was a small-scale version of large-scale filament eruptions that often involve large-scale rearrangement of coronal magnetic fields and CMEs, it is naturally expected that this eruption should be associated with a CME. We thus further examine the near-limb observations from *STEREO A*, and EUVI 304 Å and COR1 white-light images

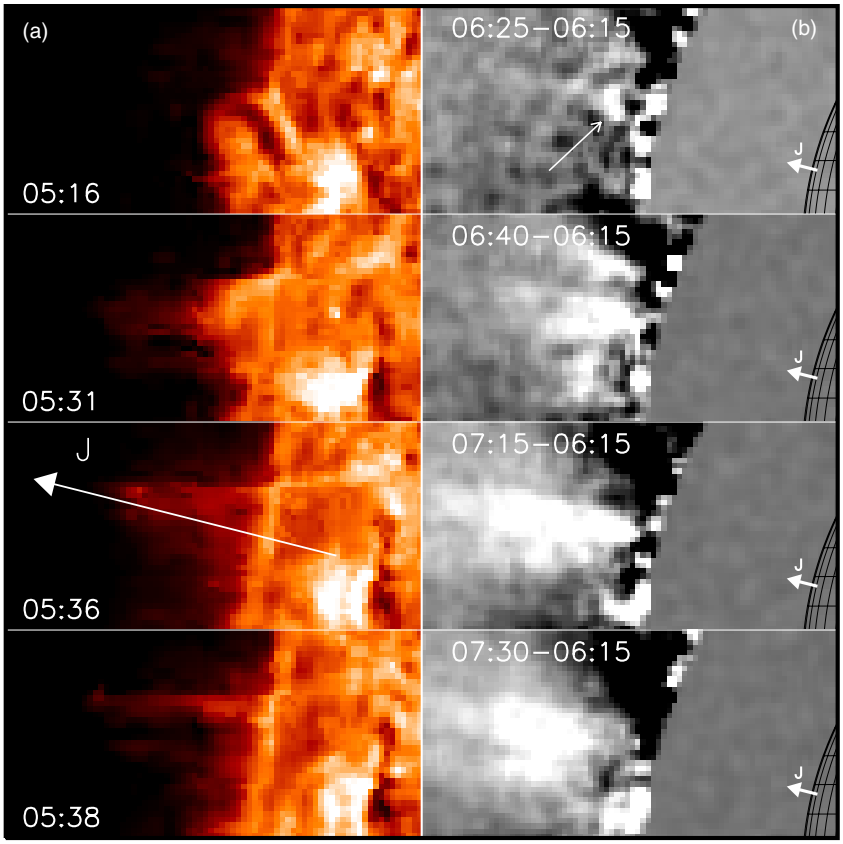

Figure 4. *STEREO A*/EUVI 304 Å direct (a) and COR1 base difference (b) images showing the near- and off-limb counterpart of the on-disk *SDO*/AIA F eruption. An EUV jet, signed by the arrow, "J," and a white-light jet directly above J can be easily identified. The FOV for panel (a) is 120″ × 60″, and it is 1180″ × 580″ for panel (b).

(A color version of this figure is available in the online journal.)

are presented in Figure 4. At 05:16 UT, the erupting 304 Å F appeared as a loop-like protrusion with a dark core above the east limb. The loop-like structure then transformed into a jet-like one that gradually faded away. Similar to the so-called blowout X-ray jets defined by Moore et al. (2010), the morphological evolution of the erupting F showed that this was a blowout EUV jet ejecting into the corona along the arrow, "J." In concert with previous results (Nistico et al. 2009; Moore et al. 2010; Raouafi et al. 2010), therefore, our observations revealed that at least part of EUV jets could have originated from eruptions of small-scale EUV filament channels. In COR1 difference images, a tiny brightening began to appear directly above the EUV jet at 06:25 UT, and then developed into a jet-like CME, i.e., a coronal white-light jet (Wang et al. 1998; Paraschiv et al. 2010). Although a larger CME event occurred to its north during this course and masked it to a certain extent, the white-light jet can be independently identified. By examining the corresponding EUV movies, no other conspicuous small eruptions were found nearby in several hours before the white-light jet. Therefore, we believe that the white-light jet was originated from the outward extension of the blowout EUV jet due to their closely spatial and temporal association. If so, our event gives the first clear example that blowout EUV jets can lead to jet-like CMEs.

4. CONCLUSIONS AND DISCUSSION

By means of the two viewpoints of observations from *SDO* and *STEREO-A*, the event was identified as a blowout EUV jet that came from the eruption of F, an EUV mini-filament channel located on the quiet Sun. The on-disk *SDO* observations clearly showed that the formation and eruption of F were similar to those of large-scale filaments in many aspects, such as the shearing, convergence, and then cancellation of opposite-polarity magnetic flux, the appearance of flare-like brightening, coronal dimming, posteruptive loops during its eruption, and so on. The near-limb *STEREO A* observations further showed that the blowout EUV jet was indeed associated with a white-light jet. In this sense, our event suggested that the eruption of an EUV mini-filament channel can actually result in a jet-like CME although it is not uncommon that EUV and white-light jets are strongly related phenomena (Wang et al. 1998; Wang & Sheeley 2002).

According to the definition of Moore et al. (2010), one unique feature of blowout jets is that the jet-base magnetic-arch core field, often carrying a filament of cool plasma, undergoes a miniature version of the blowout eruptions that produce major CMEs. Similarly, Raouafi et al. (2010) showed that coronal jets can erupt from coronal micro-sigmoids, and Nistico et al. (2009) also found some micro-CME-type jet events resembling the classical CMEs. Unlike the above observations that are mainly located in polar coronal holes, the eruption of our EUV filament channel, the on-disk counterpart of the blowout EUV jet, occurred on a quiet-Sun region near the center of the solar disk. Owing to the high spatial and temporal resolution observations of *SDO*, we can trace its entire evolution from birth to eruption, find its similarity to that of

large-scale ones, not only the eruption cause but also its outcome, and thus definitely confirm the results of Moore et al. (2010) that a blowout jet is actually the eruption of a mini-filament channel.

Differing from the so-called mini-CMEs of Innes et al. (2009) only according to their on-disk signatures, such as small-scale coronal dimmings, waves, and so on, we indeed observed that a micro-CME, the white-light jet, was originated from the blowout EUV jet, i.e., the eruption of the EUV mini-filament channel. In contrast with the results of Wang et al. (2000) that most miniature filaments erupted toward nearby strong network elements, meaning that perhaps most of their mass is transported to other magnetic structures rather than ejected into the corona, therefore, our observations strengthened the similarity of small-scale eruptions to the large-scale filament ones that produce CMEs. Since no CME-associated miniature filament eruption was reported up until now, it is necessary to further clarify the relationships between small-scale filament eruptions, blowout jets, and micro-CMEs.

This work is supported by the 973 Program (2011CB811403), by the Natural Science Foundation of China under grant 10973038, and by the Scientific Application Foundation of Yunnan Province under grants 2007A112M and 2007A115M. The AIA and HMI data used here are courtesy of *SDO* (NASA) and the AIA/HMI consortia. The EUVI and COR1 data are courtesy of *STEREO* and the SECCHI consortium. We thank the AIA, HMI, and SECCHI teams for the easy access to calibrated data.

REFERENCES

Bi, Y., Jiang, Y. C., Yang, L. H., & Zheng, R. S. 2011, New Astron., 16, 276
Boerner, P., Soufli, R., Podgorski, W., & Wolfson, C. J. 2010, AGU Fall Meeting Abstracts, 1871
Chae, J., Qiu, J., Wang, H., et al. 1999, ApJ, 513, L75
Hermans, L. M., & Martin, S. F. 1986, BAAS, 18, 991
Innes, D. E., Genetelli, A., Attie, R., & Potts, H. E. 2009, A&A, 495, 319
Jiang, Y., Chen, H., Li, K., et al. 2007, A&A, 469, 331
Jiang, Y., & Wang, J. 2001, A&A, 367, 1022
Jiang, Y., Yang, J., Zheng, R., et al. 2009, ApJ, 693, 1851
Martin, S. F. 1998, Sol. Phys., 182, 107
Moore, R. L., Cirtain, J. W., Sterling, A. C., & Falconer, D. A. 2010, ApJ, 720, 757
Nistico, G., Bothmer, V., Patsourakos, S., & Zimbardo, G. 2010, Sol. Phys., 259, 87
Paraschiv, A. R., Lacatus, D. A., Badescu, T., et al. 2010, Sol. Phys., 264, 365
Podladchikova, O., Vourlidas, A., Van der Linden, R. A. M., et al. 2010, ApJ, 709, 369
Raouafi, N.-E., Georgoulis, M. K., Rust, D. M., & Bernasconi, P. N. 2010, ApJ, 718, 981
Ren, D., Jiang, Y., Yang, J., et al. 2008, Ap&SS, 318, 141
Sakajiri, T., Brooks, D. H., Yamamoto, T., et al. 2004, ApJ, 616, 578
Schou, J., Borrero, J. M., Norton, A. A., et al. 2010, Sol. Phys., 177
Schrijver, C. J. 2010, ApJ, 710, 1480
Schwer, K., Lilly, R. B., Thompson, B. J., & Brewer, D. A. 2002, AGU Fall Meeting Abstracts, 1
Thompson, W. T., Wei, K., Burkepile, J. T., Davila, J. M., & St. Cyr, O. C. 2010, Sol. Phys., 262, 213
Wang, J., Li, W., Denker, C., et al. 2000, ApJ, 530, 1071
Wang, Y.-M., & Sheeley, N. R., Jr. 2002, ApJ, 575, 542
Wang, Y.-M., Sheeley, N. R., Jr., Socker, D. G., et al. 1998, ApJ, 508, 899
Wuelser, J.-P., Lemen, J. R., Tarbell, T. D., et al. 2004, Proc. SPIE, 5171, 111
Zirker, J. B., Martin, S. F., Harvey, K., et al. 1997, Sol. Phys., 175, 27
Zuccarello, F., Battiato, V., Contarion, L., et al. 2007, A&A, 468, 299